Lattice vibrations of the superconducting oxide spinels $(Li, Mg)_{1+x}Ti_{2-x}O_4$

1997 J. Phys.: Condens. Matter 9 10855

(http://iopscience.iop.org/0953-8984/9/49/006)

J. Phys.: Condens. Matter **9** (1997) 10855–10865. Printed in the UK PII: S0953-8984(97)85145-4

Lattice vibrations of the superconducting oxide spinels $(Li, Mg)_{1+x}Ti_{2-x}O_4$

M A Green†, M Dalton†, K Prassides†‡, P Day† and D A Neumann§

† Royal Institution of Great Britain, 21 Albemarle Street, London W1X 4BS, UK

‡ School of Chemistry, Physics and Environmental Science, Sussex University, Falmer, Brighton BN1 9QJ, UK

§ NIST Center for Neutron Research, National Institute of Standards and Technology, Gaithersburg, MD 20899, USA

Received 19 June 1997, in final form 24 September 1997

Abstract. The lattice vibrational spectra of the spinel phases, $Li_{1+x}Ti_{2-x}O_4$ ($x = 0, 0.33$) and $Li_{1-y}Mg_yTi_2O_4$ ($y = 0.1, 0.3$) (space group $Fd\bar{3}m$), have been measured as a function of temperature and composition by neutron inelastic scattering. Calculations of phonon densities of states (PDOSs) using interatomic potentials were performed and compared with the experimental data. Extensive phonon softening and hardening are observed on Li and Mg substitution throughout the energy range 10–100 meV and are discussed in terms of electron–phonon coupling and its relevance to superconductivity. The observed PDOSs show no change on cooling through the superconducting transition temperature, T_c.

1. Introduction

Electronic properties of transition metal oxides have become an intensely active area of research since the discovery of high-temperature superconductivity in layered cuprates [1]. The high transition temperatures and unconventional normal state properties in these copper oxides casts doubts on our current understanding of superconductivity, in particular, on the role of phonon mediation in the pairing of electrons into pairs. Detailed reinvestigation of other known superconducting oxides then becomes important as a comparison to the cuprates. Reduced early transition metal oxides make a large family of superconducting oxides including the tungsten and molybdenum bronzes, niobates and titanates [2].

Titanates are of particular interest as they are considered to be good examples of Mott–Hubbard insulators, in contrast to the charge-transfer insulators encountered among the late transition metal oxides such as cuprates [3]. Mixed valency phases of general formula $Li_{1+x}Ti_{2-x}O_4$ are found [4] for compositions between metallic $LiTi_2O_4$ ($x = 0$) and insulating $Li_{1.33}Ti_{1.67}O_4$ ($x = 0.333$). The d^1 (one-electron) electronic configuration of the Ti^{3+} ion contained in this system may be analogous to the d^9 (one-hole) configuration of the Cu^{2+} ion and is worthy of detailed research. Superconductivity in $Li_{1+x}Ti_{2-x}O_4$ is found at a maximum of 13 K for $x = 0.0$. Unusually, T_c varies only slightly with Ti oxidation state up to around $x \sim 0.1$, where it falls sharply with the onset of a metal–insulator transition [5, 6]. Furthermore, the apparent superconducting volume fraction varies linearly with composition, from 100% (at $x = 0$) to 0% (at $x \sim 0.15$) [6, 7]. Electronic structure calculations [8, 9] reveal that the Fermi energy, ε_F, lies within the Ti 3d t_{2g} band with the Ti 3d e_g levels being ∼1 eV higher. A gap of around 3 eV separates the broad

0953-8984/97/4910855+11$19.50

(∼5 eV) O 2p band from the conduction band. Substituting Mg^{2+} for Li^{+} in $LiTi_2O_4$ reduces T_c in proportion to the change in the lattice parameter [10]. This is unexpected since both the increase in the number of conduction electrons and the lattice parameter would be expected to reduce the bandwidth and increase the density of states (DOS) at ε_F, and, therefore, increase T_c. However, Lambert *et al* [10] suggest that electron–electron and electron–lattice interactions are important, and hence that increased localization actually reduces the density of states at the Fermi energy.

Estimates of the density of states at the Fermi level, $N(\varepsilon_F)$, differ according to the measurement technique. Thus while band structure calculations predict $N(\varepsilon_F) \approx$ 3.2–3.3 states eV^{-1}/formula unit [8, 9], values of 2.5, 3.5 and 9.2 have been obtained from photoemission [11], magnetic susceptibility [12] and normal state heat capacity [13] measurements, respectively. The origin of the electron pairing interaction causing superconductivity in $LiTi_2O_4$ remains an open question. The Debye temperature Θ_D obtained from the specific heat measurements can be used to derive the electron–phonon coupling constant within the framework of BCS weak-coupling theory [14, 15], and yields a value of $\lambda = 0.6$–0.7 [13]. However, a value of $\lambda = 1.8$, consistent with strong coupling, has been obtained from electronic specific heat measurements [8]. Furthermore, no Li isotope effect has been observed [16, 17].

In the light of these uncertainties about the mechanism of superconductivity in the $LiTi_2O_4$ system, we have carried out a detailed neutron inelastic scattering study of both the $Li_{1+x}Ti_{2-x}O_4$ ($x = 0, 0.33$) and the $Li_{1-y}Mg_yTi_2O_4$ ($y = 0, 0.1, 0.3$) series. The evolution of the scattering law, $S(Q, \omega)$, was measured as a function of both temperature and composition. In both cuprate and non-cuprate superconductors, such measurements have proven successful in the past in identifying whether phonons are coupling with electrons and how the electron–phonon coupling strength varies with energy. For example, the neutron weighted PDOS shows little difference between the superconducting and non-superconducting compositions in the $(La, Sr)_2CuO_4$ series [18] or above and below the superconducting transition temperature in $Bi_2Sr_2CaCu_2O_8$ [19]. These subtle effects seen in the cuprates are in contrast to the pronounced changes in both energy and intensity of breathing and bending modes in $(Ba, K)BiO_3$ [20–22].

2. Experimental details

Synthesis of single-phase spinel compounds proved to be challenging and previously published routes invariably led to multi-phase samples [16]. The highest-purity powder samples of $Li_{1+x}Ti_{2-x}O_4$ ($x = 0, 0.33$) and $Li_{1-y}Mg_yTi_2O_4$ ($y = 0.1, 0.3$) were prepared from mixtures of starting materials with formal stoichiometries $Li_{2-z}TiO_{3-z/2}$, $Ti_2O_{3-\delta}$ and TiO_2 only after accurate determination of both the lithium and oxygen content (z, δ) in the starting materials. In the present preparations, these values were determined to be $z = 0.22$ and $\delta = 0.12$ by atomic absorption and thermogravimetric analysis (TGA), respectively. All stoichiometric mixtures of the starting materials were wrapped in Cu foil to reduce loss of Li and heated to 860 °C for 16 hours in an atmosphere of flowing 5% H_2 in Ar. SQUID magnetometry (Quantum Design MPMS 7) was used for the characterization of the superconducting compositions. X-ray (Siemens D 500) and high-resolution neutron (BT1 diffractometer, $\lambda = 1.539$ Å (Cu(311), 14′ collimation), National Institute of Standards and Technology, Gaithersburg, MD) powder diffraction data were used in the detailed structural characterization of the samples by the Rietveld technique, using the program FULLPROF. Reflections associated with the aluminium can and cryostat tails were excluded, as well as small impurities from other oxide phases.

Inelastic neutron scattering measurements on 5–10 g samples were performed with the TFXA spectrometer at the ISIS pulsed neutron source at the Rutherford Appleton Laboratory, UK. Measurements were performed on $LiTi_2O_4$ at 4.2 and 20 K and on $Li_{1.33}Ti_{1.67}O_4$, $Li_{0.9}Mg_{0.1}Ti_2O_4$ and $Li_{0.7}Mg_{0.3}Ti_2O_4$ at 4.2 K. The samples were cooled in a continuous-flow helium 'orange' cryostat. A background was recorded, normalized and subtracted from each spectrum. The program GAUS was used to fit Gaussian curves to these experimentally obtained spectra within the program GENIE. TFXA is an inverted geometry instrument, operating at a fixed neutron final energy of $E_F \sim 4$ meV and with an initial energy analysis performed by the time-of-flight technique. For such instruments Q/ω is constant; therefore, the measured scattering law $S(Q, \omega)$ only approximates to the generalized phonon density of states. Samples were mounted in aluminium foil. Li–O, Ti–O and O–O Buckingham potentials (table 1) and an O–O spring constant of 18.41 eV Å^{-2} (as derived for other oxide systems [23]) were employed to calculate the phonon density of states and dispersion relations in $LiTi_2O_4$ using the program GULP [24]. These results enabled comparisons to be drawn with the experimental data obtained from neutron inelastic scattering and allowed assignment of the observed phonon modes.

Table 1. Interatomic potentials used in phonon calculations.

		A (eV)	ρ (Å)	C (eV Å^6)
O shell	O shell	9547.96	0.219 16	0.0
Li core	O shell	828.01	0.279 30	0.0
Ti core	O shell	2549.4	0.298 90	0.0

Interactions between two atoms i and j are described by a short-range Buckingham potential of the form $\Phi_{ij}(r_{ij}) = A\exp(-r_{ij}/\rho_{ij}) - C/r_{ij}^6$ and a long-range Coulomb interaction.

3. Results and discussion

3.1. Crystal structures

Full profile refinement gave the best fit in the $Fd\bar{3}m$ space group, corresponding to a face-centred cell containing eight formula units. In the $Fd\bar{3}m$ structure of $Li_{1-x}Ti_{2-x}O_4$, the Li and Ti atoms occupy special positions and their separation depends only on the cubic cell parameter, a. The position of the oxygen anions is determined by an additional parameter, u. Variation of u from its ideal value of 0.25 reflects the distortion of the structure to accommodate different cation radii. In addition, direct relationships exist between the bond lengths and the parameters, a and u [15]. Increasing u moves the oxygen away from the nearest tetrahedral cation along the [111] direction, expanding the LiO_4 tetrahedra and contracting the TiO_6 octahedra.

Figure 1 shows a Rietveld refinement of the neutron powder diffraction data of $LiTi_2O_4$ at 14 K which is representative of the results obtained for the $Li_{1+x}Ti_{2-x}O_4$ solid solutions. Refined parameters and goodness-of-fit factors are tabulated in table 2. Previous studies [13] have reported lithium deficiency, probably resulting from the high-temperature firings; however, no deviation from the ideal stoichiometry of lithium or any other atom was evident in the present refinements. The refined structural parameters are in good agreement with those previously reported [4, 6, 16, 25]. The refined value of $u \approx 0.263$ for $LiTi_2O_4$ at room temperature signifies a substantial compression of the Ti–O octahedra. Li substitution of Ti in $LiTi_2O_4$ to give $Li_{1.33}Ti_{1.67}O_4$ causes no structural distortion but only a small

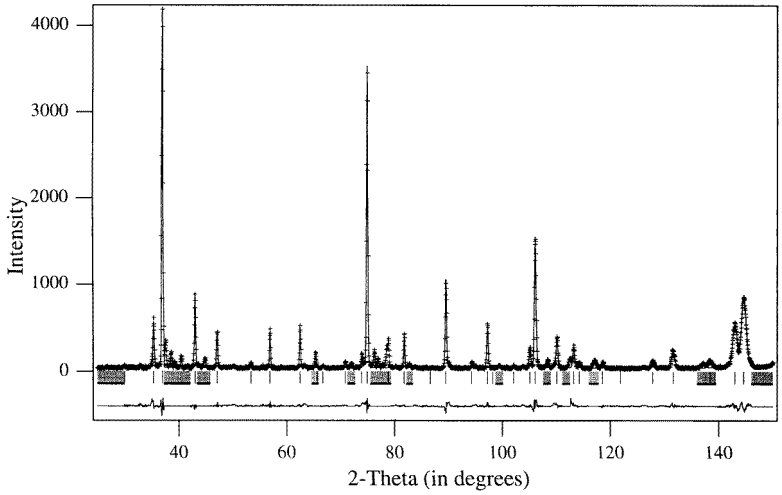

Figure 1. Observed and fitted diffraction profiles of $LiTi_2O_4$ at 14 K. The lower lines are differences between observed and calculated intensities and vertical bars indicate calculated peak positions. Regions excluded from the fits are shown hatched.

Table 2. Positional, thermal and refinement parameters for $LiTi_2O_4$ (300 K); $LiTi_2O_4$ (14 K) and $Li_{1.33}Ti_{1.67}O_4$ (300 K).

	$LiTi_2O_4$ 300 K	$LiTi_2O_4$ 14 K	$Li_{1.33}Ti_{1.67}O_4$ 300 K
a (Å)	8.409 63(7)	8.392 22(5)	8.357 14(6)
Li B (Å^2)	0.83(1)	0.35(1)	0.96(2)
Ti B (Å^2)	0.16(4)	0.11(4)	0.80(5)
O u	0.262 83(6)	0.262 70(5)	0.262 59(6)
O B (Å^2)	0.22(3)	0.17(2)	0.71(3)
χ^2	1.27	1.62	1.03
R_{wp}	12.7	11.7	12.7
R_{Bragg}	6.42	2.99	5.91

Parameters within the $Fd\bar{3}m$ spacegroup and an origin at (1/8, 1/8, 1/8). Atomic positions are Li (0.875, 0.875, 0.875), Ti (0.5, 0.5, 0.5) and O (u, u, u).

change in the parameters a and u, reflecting the similarity between the ionic radii of Ti^{4+}(octahedral) = 0.75 Å and Li^+(tetrahedral) = 0.73 Å [26].

3.2. Phonon spectra

The phonon dispersion curves and corresponding density of states calculated for $LiTi_2O_4$ are shown in figure 2(a) and (b) respectively. It is in good agreement with those calculated with a Born–von Kármán model [27] and obtained experimentally by neutron inelastic scattering in both this work and that of Gompf *et al* [27]. A short-range force constant model gave similar frequencies for zone centre vibrations [28]. We note that the $S(Q, \omega)$ measured by neutron scattering has contributions from each individual ion and is weighted by the factor (σ_i/m_i) where σ_i is the scattering cross section and m_i is the mass of atom i. The measured

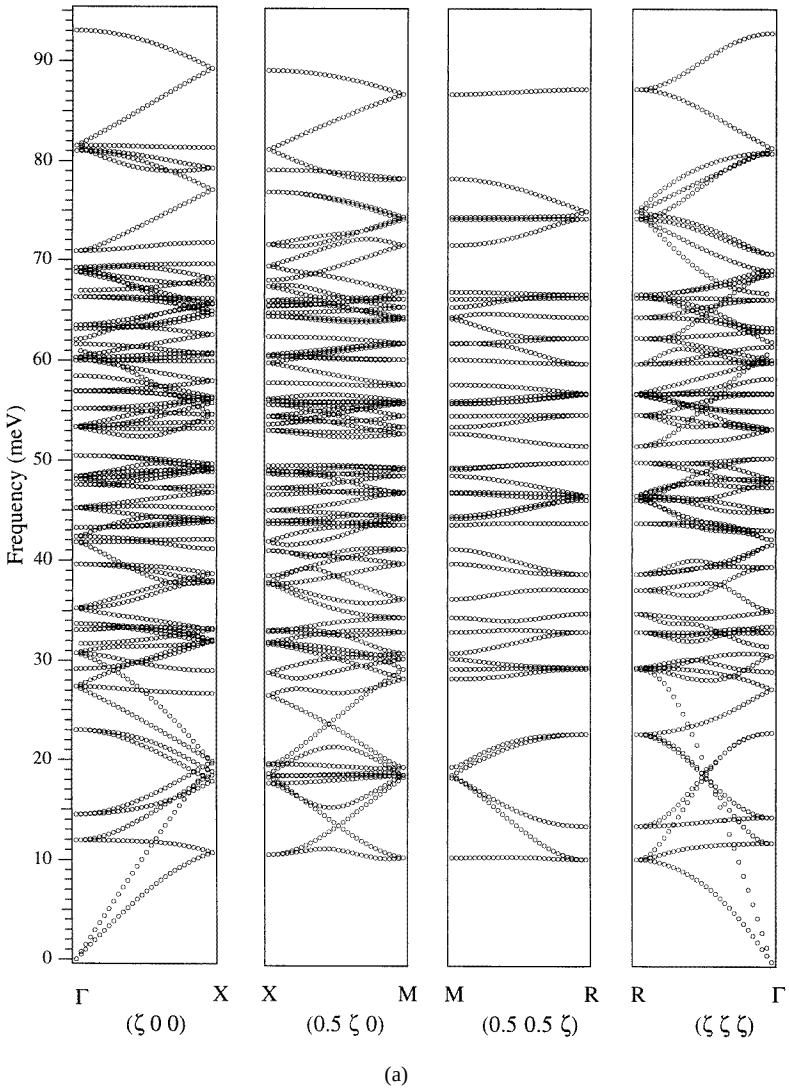

(a)

Figure 2. (a) Phonon dispersion of $LiTi_2O_4$ from Γ to X to M to R and back to Γ. (b) Phonon density of states of $LiTi_2O_4$ with the individual atom contributions shown separately.

intensities are different from those obtained in the calculations and are dominated by phonon modes which have large contributions from Li and/or O. In the calculated spectra (figure 2), the region 0 to 25 meV contains acoustic modes as well as some low-lying optical modes with Ti and O character. A peak near 30 meV with a dispersion of about 5 meV combines tetrahedral Li–O and octahedral Ti–O bending modes. Previous calculations [27] do not predict scattering in this energy range, although such scattering is observed experimentally. The region between 40 and 95 meV is dominated by O modes; contributions from Li are found at 58 and 63 meV (Li–O stretching modes) and from Ti between 55 and 80 meV (Ti–O stretching modes).

Figure 3 shows the neutron weighted phonon density of states for $LiTi_2O_4$ at 20 K and

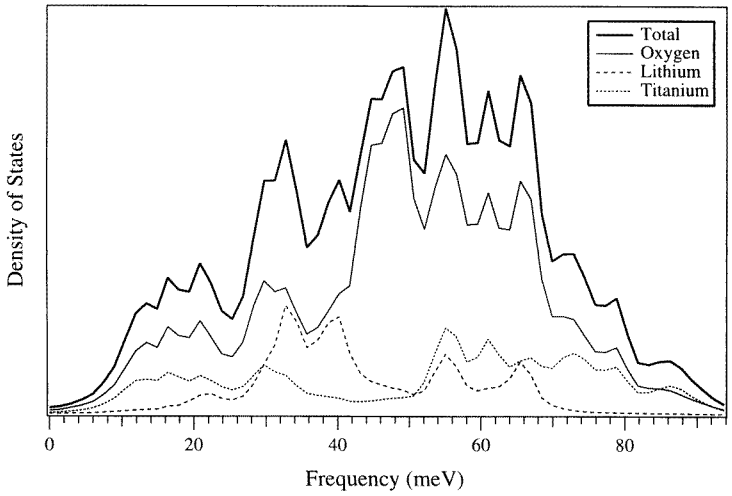

(b)

Figure 2. (Continued)

Table 3. Energies and halfwidths (FWHM) of phonon peaks in the INS spectra of $LiTi_2O_4$ (20 K); $LiTi_2O_4$ (4.2 K) and $Li_{1.33}Ti_{1.67}O_4$ (4.2 K).

$LiTi_2O_4$ 20 K		$LiTi_2O_4$ 4.2 K		$Li_{1.33}Ti_{1.67}O_4$ 4.2 K	
(FWHM) (meV)	Frequency (meV)	(FWHM) (meV)	Frequency (meV)	(FWHM) (meV)	Frequency (meV)
2.1(2)	12.1(1)	2.1(2)	12.4(1)	3.1(1)	12.1(2)
1.6(1)	13.0(2)	1.4(3)	13.2(3)	1.6(2)	13.0(1)
2.0(2)	15.2(2)	1.4(3)	15.4(3)	2.0(3)	15.4(2)
2.5(2)	19.1(2)	2.9(2)	19.1(2)	2.3(2)	19.3(4)
5.0(3)	22.1(2)	2.1(3)	22.1(2)	3.4(4)	22.9(3)
4.0(2)	27.0(1)	5.5(2)	26.4(2)	1.9(2)	26.5(3)
2.4(1)	33.9(2)	3.1(2)	34.1(1)	7.3(2)	31.9(2)
12.2(1)	44.6(2)	10.2(2)	44.0(3)	3.2(3)	36.5(2)
1.3(2)	52.1(2)	1.7(1)	52.3(2)	9.3(2)	42.8(2)
7.6(3)	56.7(1)	14.2(1)	56.1(2)	4.2(1)	49.9(2)
6.9(4)	63.2(1)	4.9(3)	63.3(3)	8.5(3)	57.2(2)
8.5(4)	72.1(2)	7.5(2)	70.8(2)	6.5(2)	73.3(2)
15.3(7)	88.2(2)	22.5(2)	89.8(2)	3.5(2)	84.0(4)
10.8(5)	102.8(3)	8.7(1)	103.0(2)	7.8(2)	91.6(6)
				6.4 (3)	103.8 (3)

4.2 K as well as $Li_{1.33}Ti_{1.67}O_4$ at 4.2 K. In both phases the scattering between 45 and 60 meV is dominated by a single broad feature centred near 52 meV, though in the superconducting $LiTi_2O_4$ compound there is an additional shoulder at 47 meV. The calculations predict that the scattering in this region originates almost entirely from O vibrations. Scattering below 45 meV should contain significant contributions from both Li and Ti but the resolution does not allow a more detailed analysis. The most striking difference between the two compounds is the reduction of scattering intensity between 60 and 66 meV in insulating $Li_{1.33}Ti_{1.67}O_4$, while the spectra of both compounds are similar above 70 meV.

Table 3 lists the peak energies and FWHM obtained from Gaussian fits to individual features in the spectra. In contrast to the pronounced changes found in $(Ba, K)BiO_3$ [20],

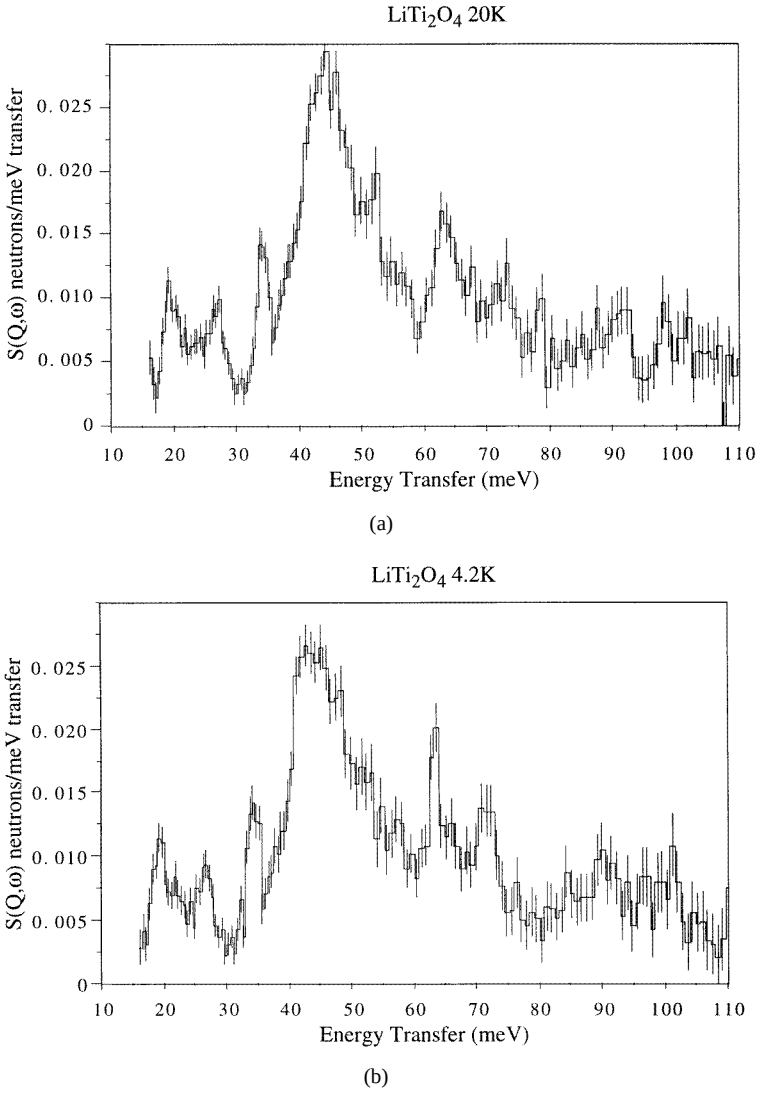

Figure 3. Observed neutron weighted phonon density of states of (a) $LiTi_2O_4$ at 20 K, (b) $LiTi_2O_4$ at 4.2 K and (c) $Li_{1.33}Ti_{1.67}O_4$ at 4.2 K.

there is no change in either energy or width for any of the vibrational peaks, within the resolution of the instrument, on cooling $LiTi_2O_4$ from 20 K through the superconducting transition temperature to 4.2 K. The absence of changes does not rule out a BCS-like mechanism for superconductivity in $LiTi_2O_4$ because the large number of phonon modes in the spinel structure may make changes to strongly coupled phonons difficult to detect.

There are considerable differences between the vibrational spectra of superconducting $LiTi_2O_4$ and insulating $Li_{1.33}Ti_{1.67}O_4$. The peaks at 19, 22 and 26 meV, originating from O modes with a substantial amount of Li character, are unchanged. However, the peak at 26 meV overlaps with the large dispersion from the mode centred at 31.9 meV. The width of the latter increases from 3.1 meV in $LiTi_2O_4$ to 7.3 meV in $Li_{1.33}Ti_{1.67}O_4$. Calculations

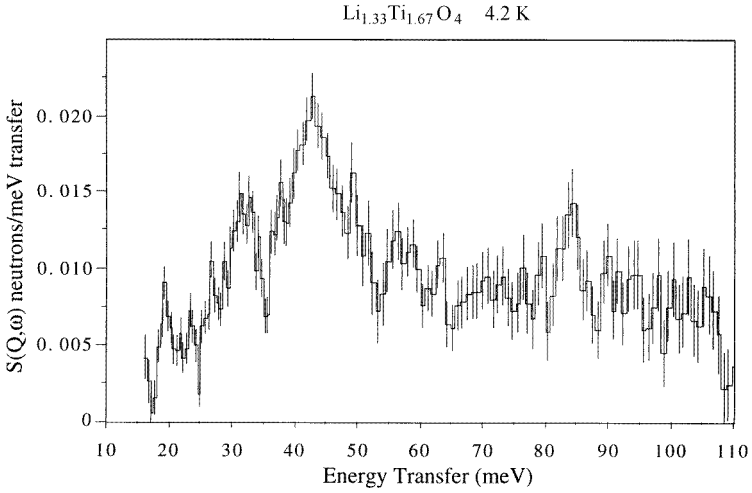

(c)

Figure 3. (Continued)

predict that this peak is a combination of tetrahedral and octahedral modes with significant contributions from Li, Ti and O atoms. The increase in scattering can be accounted for by the direct substitution of Li for Ti since the former has a larger scattering cross-section while the broadening reflects disorder. The peak at 42.8 meV in $Li_{1.33}Ti_{1.67}O_4$ shifts to 44.0 meV in $LiTi_2O_4$ and decreases in intensity, in agreement with previous results [27]. Between 54 and 80 meV, all three peaks broaden, but do not shift. An increase in relative intensity at 84 meV arises from the increased intensity of the octahedral breathing mode on substituting Li for Ti. The high-frequency modes at 90 and 103 meV also soften. Substituting Li for Ti causes a 10% reduction in the mass of the MO_6 octahedral unit. It is possible that the softening of the high-frequency phonons above 84 meV in $LiTi_2O_4$ compared with $Li_{1.33}Ti_{1.67}O_4$ is simply due to this change in mass. On the other hand the increase in the energy of the phonon modes between 37 and 54 meV in $LiTi_2O_4$ compared with $Li_{1.33}Ti_{1.67}O_4$ cannot be easily rationalized due to substitution of a lighter ion. Electron–phonon interaction in a superconductor has a major effect on its phonon energies. Within the framework of a conventional BCS mechanism, phonons in superconductors are characteristically shifted compared to those in similar non-superconducting compositions. This shift is dependent on the value of the electron–phonon coupling constant and the difference in energy between a particular phonon and the superconducting energy gap [29]. In the case of $(Ba, K)BiO_3$, two particular phonon modes at 33 meV (oxygen bending) and at 62 meV (oxygen stretching) are found to shift significantly with composition. Furthermore, a temperature effect above and below the superconducting transition temperature unambiguously identifies these modes as displaying strong electron–phonon coupling. In contrast, the results reported above for the $Li_{1+x}Ti_{2-x}O_4$ system seem to indicate a quite different coupling scheme. Although phonon softening and hardening are clearly identified with changes in composition, giving direct evidence of strong electron–phonon coupling, there are no clear phonon modes which are affected, but rather a continuous range of phonon energies.

Figures 4(a) and 4(b) show the neutron weighted phonon density of states for the Mg substituted compounds, $Li_{0.9}Mg_{0.1}Ti_2O_4$ and $Li_{0.7}Mg_{0.3}Ti_2O_4$, at 4.2 K. Mg substitution has only a subtle effect on the vibrational spectra. The increased mass of the tetrahedral

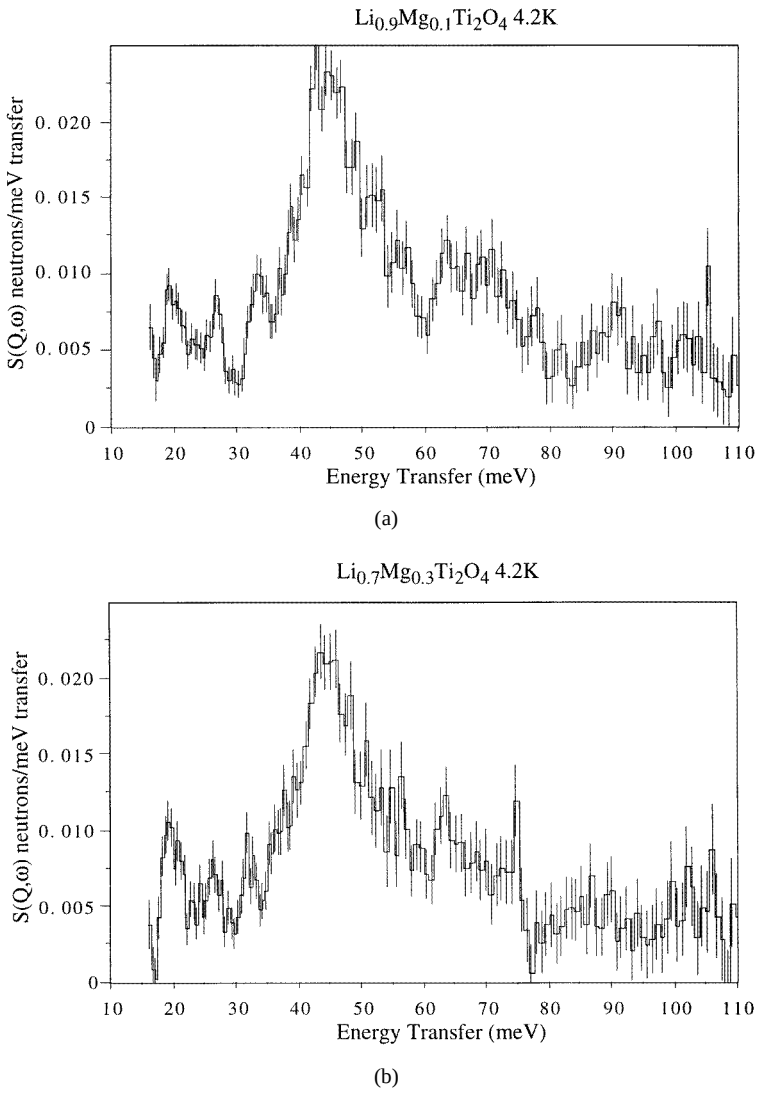

Figure 4. Observed neutron weighted phonon density of states of (a) $Li_{0.9}Mg_{0.1}Ti_2O_4$ and (b) $Li_{0.7}Mg_{0.3}Ti_2O_4$ at 4.2 K.

unit explains the shifts in vibrations at 34.1 meV and 89.8 meV in $LiTi_2O_4$ to 33.2 meV and 89.2 meV in $Li_{0.9}Mg_{0.1}Ti_2O_4$, and 31.7 meV and 86.0 meV in $Li_{0.7}Mg_{0.3}Ti_2O_4$. It is noteworthy that, compared to $Li_{1.33}Ti_{1.67}O_4$, the Mg substituted materials still show characteristics attributed to strong electron–phonon coupling, as described for $LiTi_2O_4$, making the reduction of T_c more difficult to understand.

4. Conclusions

High-resolution powder neutron diffraction confirms that all $Li_{1+x}Ti_{2-x}O_4$ phases share the $Fd\bar{3}m$ spinel structure from $x = 0$ to 0.33. However, the addition of Li to $LiTi_2O_4$

introduces structural disorder, revealed in large thermal parameters for the (Ti, Li) and O atoms (see table 2) and broadening of a number of vibrational peaks. The disorder arises from discrete Ti^{4+} and Li^{+} ions, leading to a wide range of bond lengths between O and the (Ti, Li) sites. Inelastic neutron scattering measurements of the vibrational spectra were performed across the regions of temperature and composition in the phase diagram that encompass the metallic, superconducting and insulating regimes. There is no discernible difference in any of the vibrational features of $LiTi_2O_4$ between the superconducting (4.2 K) and normal state (20 K). However, there are pronounced differences between the phonon spectra of superconducting $LiTi_2O_4$ with insulating $Li_{1.33}Ti_{1.67}O_4$, indicating strong electron–phonon coupling and providing evidence for BCS-like phonon mediated superconductivity. The conduction band of $LiTi_2O_4$ is largely composed of Ti states, so that Ti vibrations might be considered to be more strongly coupled to the electronic system. Titanium vibrations are calculated to have substantial contributions throughout the whole range of the phonon spectra. Therefore, the large range in which the phonon anomalies are observed might be expected. Superconductivity in elements and alloys is associated with coupling to a particular acoustic mode, close in energy to the superconducting gap. It is important to note that $LiTi_2O_4$ shows vibrations typical of those involved in strong electron–phonon coupling at energies very different from the superconducting gap energy.

Acknowledgments

We acknowledge the UK Engineering and Physical Sciences Research Council for financial support and a Research Fellowship (MD) and Research Studentship (MAG). Thanks are due to the National Institute of Standards and Technology and ISIS for access to neutron beam facilities. We thank J J Rush and J K Stalick for many useful discussions.

References

[1] Bednorz J G and Muller K A 1986 *Z. Phys.* B **64** 189
[2] Etourneau J 1992 *Solid State Chemistry: Compounds* ed A K Cheetham and P Day (Oxford: Clarendon) p 60
[3] Fujimori A and Tokura Y 1995 *Spectroscopy of Mott Insulators and Correlated Metals* (Berlin: Springer)
[4] Deschanvres A, Raveau B and Sekkal Z 1971 *Mater. Res. Bull.* **6** 699
[5] Johnston D C, Prakash H, Zachariasen W H and Vishwanathan R 1973 *Mater. Res. Bull.* **8** 777
[6] Johnston D C 1976 *J. Low Temp. Phys.* **25** 145
[7] Harrison M R, Edwards P P and Goodenough J B 1985 *Phil. Mag.* B **52** 679
[8] Satpathy S and Martin R M 1987 *Phys. Rev.* B **36** 11 352
[9] Massidda S, Yu J J and Freeman A J 1988 *Phys. Rev.* B **38** 11 352
[10] Lambert P M, Harrison M R, Logan D E and Edwards P P 1987 *Disordered Semi-conductors* ed M A Kastner, G A Thomas and S R Orshinsky (New York: Plenum) p 135
[11] Edwards P P, Egdell R G, Fragala I, Goodenough J B, Harrison M R, Orchard A F and Scott E G 1984 *J. Solid State Chem.* **54** 127
[12] Watanbe M, Kaneda K, Takeda H and Tsuda N 1984 *J. Phys. Soc. Japan* **53** 2437
[13] McCallum R W, Johnston R C, Luengo C A and Maple M B 1976 *J. Low Temp. Phys.* **25** 177
[14] McMillan W L 1968 *Phys. Rev.* **167** 331
[15] Hill R J, Craig J R and Gibbs G V 1979 *Phys. Chem. Miner.* **4** 317
[16] Dalton M 1992 *PhD Thesis* Cambridge University
[17] Goodrich R G 1991 *Phys. Rev.* B **44** 5326
[18] Rosseinsky M J, Prassides K, Day P and Dianoux A J 1988 *Phys. Rev.* B **37** 2231
[19] Renker B, Gompf F, Gering E, Ewert D, Rietschel H and Dianoux A J 1988 *Z. Phys.* B **73** 309
[20] Green M A, Prassides K, Neumann D A and Day P 1995 *Chem. Mater.* **7** 888
[21] Prassides K, Rosseinsky M J, Dianoux A J and Day P 1992 *J. Phys.: Condens. Matter* **4** 965

[22] Loong C, Hinks D G, Vashishta P, Jin W, Kalia R K, Degani M H, Price D L, Jorgensen J D, Dabrowski B, Michell A W, Richard D R and Zheng Y 1991 *Phys. Rev. Lett.* **66** 3217
[23] Lewis D and Catlow C R A 1986 *J. Phys. Chem. Solids* **47** 89
[24] J. Gale *GULP* (London: The Royal Institution of Great Britain and Imperial College) (1992–1997)
[25] Cava R J, Murphy D W, Zahurak S, Santoro A and Roth R S 1984 *J. Solid State Chem.* **53** 64
[26] Shannon R D 1976 *Acta Crystallogr.* A **32** 751
[27] Gompf F, Renker B and Mutka H 1992 *Physica* B **180** 459
[28] Gupta H C and Ashdir P 1997 *Physica* B **233** 213
[29] Zeyher R and Zwicknagl G 1990 *Z. Phys.* B **78** 175